

# Classical Density Functional Theory for Particles with Hard Cores and Soft Square Shoulders

Bachelorarbeit aus der Physik

Vorgelegt von  
**Markus Hoffmann**

22.10.2019

Institut für Theoretische Physik I  
Friedrich-Alexander-Universität Erlangen-Nürnberg



Betreuer: Prof. Dr. Michael Schmiedeberg



## Abstract

Classical density functional theory is an excellent tool to investigate classical many-body systems from fundamental principles, in particular soft matter systems. Here we consider hard particles with soft square shoulders in two dimensions. Since two mesoscopic particles cannot be at the same position at the same time, hard particles are a suitable model system. We model the interaction of impenetrable particles via infinite potentials. By adding soft shoulders, which are modelled by finite step potentials, we obtain a second length scale in our system. Two different length scales often lead to interesting pattern formations such as simple quadratic phases and quasiperiodic crystals. In this bachelor's thesis we recover the liquid-solid phase transition for hard particles and for soft particles.



## Acknowledgements

I would like to sincerely thank Prof. Michael Schmiedeberg for the excellent supervision of this bachelor's thesis, especially for the many helpful personal conversations and discussions on physics and for the valuable guidance. With an open office door, he was always approachable for questions.

Moreover, I truly thank Robert Weigel for his great support, in particular during the numerical implementation.



# Contents

<b>1</b>	<b>Motivation</b>	<b>1</b>
<b>2</b>	<b>Theoretical Background</b>	<b>2</b>
2.1	Statistical Physics Background . . . . .	3
2.2	Density Functional Theory . . . . .	4
2.3	Fundamental Measure Theory for Hard Disks . . . . .	6
2.4	Coarse-Grained Free Energy Functional for Soft Particles . . . . .	8
<b>3</b>	<b>Numerical Calculations</b>	<b>10</b>
3.1	Box . . . . .	10
3.2	Initial Density Field . . . . .	11
3.3	Weight Functions $\omega_\nu(\mathbf{r})$ . . . . .	11
3.4	Weight Functions $n_\nu(\mathbf{r})$ . . . . .	13
3.5	Weight Functions $T_\nu(\mathbf{r})$ . . . . .	13
3.6	Functional Derivative of Excess Free Energy for Hard Particles . . . . .	14
3.7	Functional Derivative of Excess Free Energy for Soft Particles . . . . .	14
3.8	Picard Iteration . . . . .	15
<b>4</b>	<b>Results</b>	<b>16</b>
4.1	Test Case: Weight Functions $\omega_\nu(\mathbf{r})$ . . . . .	16
4.2	Test Case: Constant Density Field . . . . .	17
4.3	Test Case: Freezing Transition of Hard Disks in Two Dimensions . . . . .	18
4.4	Test Case: Freezing Transition of Soft Disks in Two Dimensions . . . . .	20
4.5	Hard Core and Soft Shoulders . . . . .	21
4.6	Interesting Patterns . . . . .	23
<b>5</b>	<b>Resume and Outlook</b>	<b>25</b>
<b>6</b>	<b>References</b>	<b>26</b>
<b>7</b>	<b>Appendix</b>	<b>28</b>



# 1 Motivation

Pierre-Gilles de Gennes applied the concepts of thermodynamics to complex soft matter systems. In 1991 he received the Nobel Prize in Physics for discovering that methods developed for studying order phenomena in simple systems can be generalized to more complex forms of matter, in particular to liquid crystals and polymers [1]. Soft matter is a subfield of condensed matter and deals with a class of materials which include polymers, colloids, surfactants and liquid crystals. A common feature of all soft matter systems is their structure consisting of large elements such as macromolecules, colloidal particles, molecular assemblies or ordered molecules. The typical length scales of soft matter are between  $0.01 \mu m$  and  $100 \mu m$ . Since this scale is much larger than the length scales of electrons and atoms, quantum mechanics can be neglected [2].

One of the simplest model systems to describe soft matter are hard disks. Hard disks are impenetrable and do not interact if their distance is larger than their diameter. For such systems the liquid-solid phase transition is purely entropically driven.

In 1964 density functional theory was introduced by Hohenberg and Kohn as a method to describe the inhomogeneous electron gas at temperature  $T = 0 K$  with a functional for the energy that only depends on the electron density [3]. In 1998 Kohn received the Nobel Prize in Chemistry for his development of density functional theory [4]. In 1965 Mermin extended this method to nonzero temperatures  $T > 0 K$  [5].

Classical density functional theory describes both hard disks based on Rosenfeld's fundamental measure theory [6] and soft disks based on a mean field approximation [7]. The main challenge is to find a functional that describes the particle interactions and the phase transitions. In 1989 Rosenfeld introduced a new method to construct density functional theory for hard sphere mixtures. This method uses fundamental geometric properties of individual spheres and is called fundamental measure theory. The approach of Rosenfeld describes three-dimensional systems correctly but fails to describe two-dimensional systems [8, 9]. Therefore we will use the approach [9] outlined by Tarazona and Rosenfeld [10, 11] which correctly describes the hard disk solid phase.

## 2 Theoretical Background

In this chapter we will provide a brief review, in which we cover classical statistical physics of interacting particles, introduce classical density functional theory, and construct an excess free energy functional for hard disks in two dimensions via fundamental measure theory. Moreover we will provide a coarse-grained mean field approximation for finite potentials and combine the infinite step potential for hard particles with a finite step potential for soft particles as shown in figure 1. This models particles with hard cores and soft shoulders as shown in figure 2.

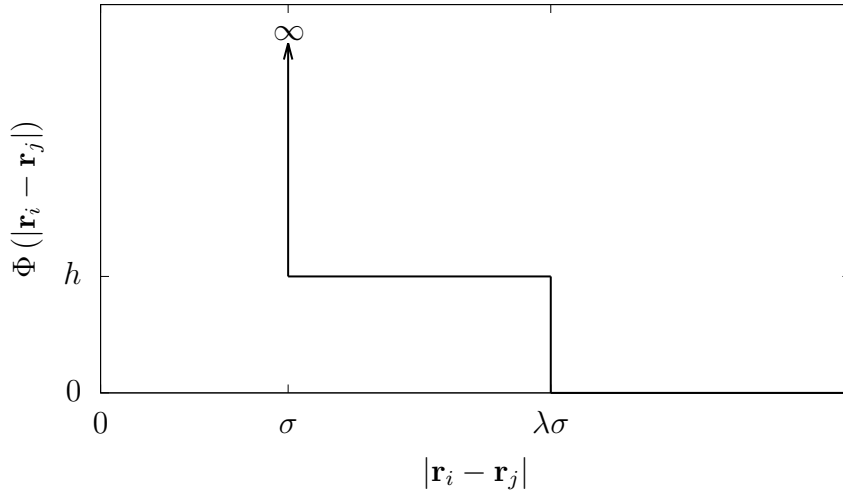


Figure 1: Potential to model the pairwise interaction between particles  $i$  and  $j$  given their positions  $\mathbf{r}_i$  and  $\mathbf{r}_j$ . This potential models particles with hard cores of diameter  $\sigma$  and soft shoulders of height  $h$  and diameter  $\lambda\sigma$ . This potential is described by three positive real parameters  $\sigma$ ,  $h$  and  $\lambda$  with  $\lambda > 1$ .

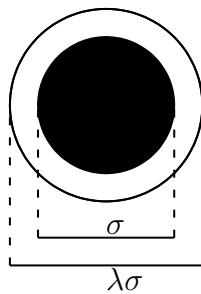


Figure 2: Particle with a hard core of diameter  $\sigma$  and larger soft shoulders of diameter  $\lambda\sigma$  with  $\lambda > 1$ .

The ideas presented in the following subsections are based on the PhD thesis [12], the review articles [13, 14], and the lecture notes [15, 16].

## 2.1 Statistical Physics Background

In the following section we will introduce the essentials of classical equilibrium statistical physics which are required for density functional theory.

We consider a system of  $N$  identical classical particles in two dimensions. Therefore, this system is described by  $4N$  coordinates, composed of  $2N$  coordinates for the position of each particle and  $2N$  coordinates for the momentum of each particle. The ensemble of the positions of all particles will be labelled  $\{\mathbf{r}_i\}$ , the ensemble of the momenta of all particles will be labelled  $\{\mathbf{p}_i\}$  and the ensemble of the positions and the momenta of all particles will be labelled  $\boldsymbol{\pi} = \{\mathbf{r}_i, \mathbf{p}_i\}$  with  $i = 1, \dots, N$ . The Hamiltonian for this system is given as

$$\begin{aligned} H(\boldsymbol{\pi}) &= T(\{\mathbf{p}_i\}) + U(\{\mathbf{r}_i\}) \\ &= T(\{\mathbf{p}_i\}) + U_{\text{int}}(\{\mathbf{r}_i\}) + U_{\text{ext}}(\{\mathbf{r}_i\}) \end{aligned} \quad (1)$$

with the kinetic energy

$$T(\{\mathbf{p}_i\}) = \sum_{i=1}^N \frac{\mathbf{p}_i^2}{2m_i}. \quad (2)$$

While  $m_i$  is the mass of particle  $i$ , the potential energy is given by  $U(\{\mathbf{r}_i\})$  and will be split into two terms. The potential energy due to pairwise particle interactions is described with an interaction potential  $\Phi(\mathbf{r}_i, \mathbf{r}_j)$  for particles  $i$  and  $j$  as

$$U_{\text{int}}(\{\mathbf{r}_i\}) = \sum_{i=1}^N \sum_{j=1}^{i-1} \Phi(\mathbf{r}_i, \mathbf{r}_j). \quad (3)$$

The potential energy due to an external potential  $V(\mathbf{r})$  is given by

$$U_{\text{ext}}(\{\mathbf{r}_i\}) = \sum_{i=1}^N V(\mathbf{r}_i). \quad (4)$$

Solving the Hamiltonian for many body systems consisting of large numbers of particles is hardly possible due to its complexity. Therefore we introduce macroscopic variables to describe the physical system in a coarse-grained manner which is the domain of thermodynamics and statistical mechanics. Depending on the variables we introduce in order to describe our system, there are different ensembles. The canonical ensemble describes systems with fixed temperature  $T$ , fixed volume  $V$  and a fixed number of particles  $N$  by the canonical partition function

$$Z(T, V, N) = \frac{1}{h^{2N} N!} \int_{\mathbb{R}^{4N}} \prod_{i=1}^N d\mathbf{r}_i d\mathbf{p}_i \exp(-\beta H(\boldsymbol{\pi})). \quad (5)$$

Hereby  $h$  denotes the Planck constant and  $\beta = (k_B T)^{-1}$  the inverse temperature with the Boltzmann constant  $k_B$ . The Helmholtz free energy is given by

$$F(T, V, N) = -k_B T \ln(Z(T, V, N)) . \quad (6)$$

For a potential of the form  $U(\{\mathbf{r}_i\})$ , which only depends on the positions of the particles, the integration of the momenta can be calculated directly. In consequence the canonical partition function simplifies to

$$Z(T, V, N) = \frac{1}{\Lambda^{2N} N!} \int_{\mathbb{R}^{2N}} \prod_{i=1}^N d\mathbf{r}_i \exp(-\beta U(\{\mathbf{r}_i\})) \quad (7)$$

with the thermal de Broglie wavelength  $\Lambda = h/\sqrt{2\pi m k_B T}$ .

The grand canonical ensemble for systems with fixed temperature  $T$ , fixed volume  $V$  and fixed chemical potential  $\mu$  is described by the grand canonical partition function

$$\Xi(T, V, \mu) = \sum_{N=0}^{\infty} z^N Z(T, V, N) = \sum_{N=0}^{\infty} \frac{z^N}{h^{2N} N!} \int_{\mathbb{R}^{4N}} \prod_{i=1}^N d\mathbf{r}_i d\mathbf{p}_i \exp(-\beta H(\boldsymbol{\pi})) \quad (8)$$

with the fugacity  $z = \exp(\beta\mu)$ . The grand canonical free energy is

$$\Omega(T, V, \mu) = -k_B T \ln(\Xi(T, V, \mu)) . \quad (9)$$

In the grand canonical ensemble, the average of any observable  $O(\boldsymbol{\pi})$  is defined as

$$\langle O(\boldsymbol{\pi}) \rangle = \frac{1}{\Xi(T, V, \mu)} \sum_{N=0}^{\infty} \frac{z^N}{h^{2N} N!} \int_{\mathbb{R}^{4N}} \prod_{i=1}^N d\mathbf{r}_i d\mathbf{p}_i O(\boldsymbol{\pi}) \exp(-\beta H(\boldsymbol{\pi})) . \quad (10)$$

## 2.2 Density Functional Theory

In the microscopic description of our system, the microscopic one-body density is defined by the positions of the particles as  $\sum_{i=1}^N \delta(\mathbf{r} - \mathbf{r}_i)$ . The average one-body density can be calculated for any given microscopic density as the grand canonical average of the microscopic density

$$\rho(\mathbf{r}) = \left\langle \sum_{i=1}^N \delta(\mathbf{r} - \mathbf{r}_i) \right\rangle . \quad (11)$$

In [5] it has been shown that the grand canonical free energy  $\Omega$  is a unique functional of the average one-body density and that this unique functional becomes minimal for the equilibrium one-body density  $\rho_{\text{equ}}(\mathbf{r})$ . This implies

$$\left. \frac{\delta\Omega[\rho(\mathbf{r})]}{\delta\rho(\mathbf{r})} \right|_{\rho(\mathbf{r})=\rho_{\text{equ}}(\mathbf{r})} = 0 . \quad (12)$$

Via a Legendre transformation we obtain the Helmholtz free energy functional

$$F[\rho(\mathbf{r})] = \Omega[\rho(\mathbf{r})] + \mu \int_{\mathbb{R}^2} d\mathbf{r} \rho(\mathbf{r}) . \quad (13)$$

We introduce the intrinsic Helmholtz free energy functional which is independent of an external potential  $V(\mathbf{r})$  as

$$\mathcal{F}[\rho(\mathbf{r})] = F[\rho(\mathbf{r})] - \int_{\mathbb{R}^2} d\mathbf{r} \rho(\mathbf{r}) V(\mathbf{r}) \quad (14)$$

and decompose  $\mathcal{F}[\rho(\mathbf{r})]$  into a sum of an ideal gas term and an excess term due to interparticle interactions that exceed an ideal gas. Furthermore the excess term will be split into hard core interactions and into soft square shoulder interactions as

$$\begin{aligned} \mathcal{F}[\rho(\mathbf{r})] &= \mathcal{F}_{\text{id}}[\rho(\mathbf{r})] + \mathcal{F}_{\text{exc}}[\rho(\mathbf{r})] \\ &= \mathcal{F}_{\text{id}}[\rho(\mathbf{r})] + \mathcal{F}_{\text{exc,hard}}[\rho(\mathbf{r})] + \mathcal{F}_{\text{exc,soft}}[\rho(\mathbf{r})] . \end{aligned} \quad (15)$$

The free energy of an ideal gas in two dimensions is given by

$$\mathcal{F}_{\text{id}}[\rho(\mathbf{r})] = \beta^{-1} \int_{\mathbb{R}^2} d\mathbf{r} \rho(\mathbf{r}) [\ln(\Lambda^2 \rho(\mathbf{r})) - 1] . \quad (16)$$

So far we have rewritten the grand canonical free energy as

$$\begin{aligned} \Omega[\rho(\mathbf{r})] &= \beta^{-1} \int_{\mathbb{R}^2} d\mathbf{r} \rho(\mathbf{r}) [\ln(\Lambda^2 \rho(\mathbf{r})) - 1 + \beta V(\mathbf{r}) - \beta \mu] \\ &\quad + \mathcal{F}_{\text{exc,hard}}[\rho(\mathbf{r})] + \mathcal{F}_{\text{exc,soft}}[\rho(\mathbf{r})] . \end{aligned} \quad (17)$$

The equilibrium density profile  $\rho_{\text{equ}}(\mathbf{r})$  is given by the minimum of the grand canonical potential

$$\left. \frac{\delta \Omega[\rho(\mathbf{r})]}{\delta \rho(\mathbf{r})} \right|_{\rho(\mathbf{r})=\rho_{\text{equ}}(\mathbf{r})} \stackrel{!}{=} 0 . \quad (18)$$

Calculating the functional derivative of the grand canonical free energy leads to

$$\frac{\delta \Omega[\rho(\mathbf{r})]}{\delta \rho(\mathbf{r})} = \frac{\delta \mathcal{F}_{\text{exc,hard}}[\rho(\mathbf{r})]}{\delta \rho(\mathbf{r})} + \frac{\delta \mathcal{F}_{\text{exc,soft}}[\rho(\mathbf{r})]}{\delta \rho(\mathbf{r})} + \beta^{-1} \ln(\Lambda^2 \rho(\mathbf{r})) + V(\mathbf{r}) - \mu . \quad (19)$$

Therefore we obtain the following equation for the equilibrium density

$$\rho(\mathbf{r}) = \frac{1}{\Lambda^2} \exp \left( - \frac{\delta(\beta \mathcal{F}_{\text{exc,hard}}[\rho(\mathbf{r})])}{\delta \rho(\mathbf{r})} - \frac{\delta(\beta \mathcal{F}_{\text{exc,soft}}[\rho(\mathbf{r})])}{\delta \rho(\mathbf{r})} - \beta V(\mathbf{r}) + \beta \mu \right) . \quad (20)$$

The functional derivative of the excess free energy can be generalised to higher order functional derivatives. Those are called direct correlation functions and are defined as

$$\begin{aligned} c^{(1)}(\mathbf{r}) &:= - \frac{\delta(\beta \mathcal{F}_{\text{exc}}[\rho(\mathbf{r})])}{\delta \rho(\mathbf{r})} \\ c^{(n)}(\mathbf{r}_1, \dots, \mathbf{r}_n) &:= - \frac{\delta c^{n-1} \rho(\mathbf{r}_1, \dots, \mathbf{r}_{n-1})}{\delta \rho(\mathbf{r}_n)} . \end{aligned} \quad (21)$$

So far, no approximations were introduced by density functional theory. Now, the task is to determine the excess free energy functional  $\mathcal{F}_{\text{exc,hard}}[\rho(\mathbf{r})]$  and  $\mathcal{F}_{\text{exc,soft}}[\rho(\mathbf{r})]$  in the following two sections.

## 2.3 Fundamental Measure Theory for Hard Disks

The fundamental measure theory is a mean-field approximation, which only depends on the density field but not on density correlations or fluctuations. In the following we will consider an ensemble of identical hard disks in a two-dimensional system without any external potential. The disks with diameter  $\sigma$  interact according to a hard-body pair-potential

$$\Phi_{\text{hard}}(\mathbf{r}_i, \mathbf{r}_j) = \begin{cases} \infty & , \text{for } |\mathbf{r}_i - \mathbf{r}_j| < \sigma \\ 0 & , \text{otherwise} \end{cases} \quad (22)$$

as shown in figure 3.

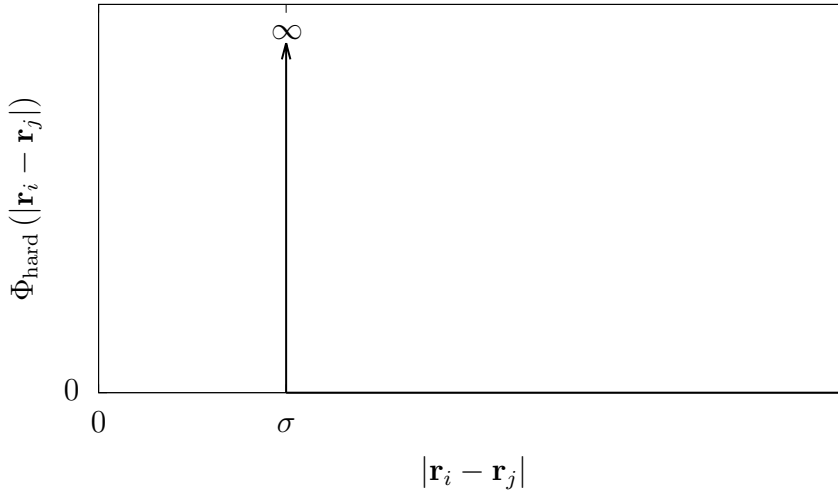


Figure 3: Potential to model the pairwise interaction between particles  $i$  and  $j$  given their positions  $\mathbf{r}_i$  and  $\mathbf{r}_j$ . This potential models particles with hard cores of diameter  $\sigma$ . This potential is described by one positive real parameter  $\sigma$ .

We introduce  $r$  as the distance  $|\mathbf{r}_i - \mathbf{r}_j|$  between the two position vectors of disk  $i$  and disk  $j$ . The Mayer function  $f(r) = \exp(-\beta\Phi(r)) - 1$  for the potential given in equation 22 can be expressed as

$$f(r) = \begin{cases} -1 & , \text{for } r < \sigma \\ 0 & , \text{otherwise} \end{cases} \quad (23)$$

The Heaviside step function  $\Theta(r)$  is defined by

$$\Theta(r) = \begin{cases} 1 & , \text{for } r > 0 \\ 0 & , \text{for } r \leq 0 \end{cases} . \quad (24)$$

Hence the Mayer function can be written as

$$f(r) = -\Theta(\sigma - r) \quad (25)$$

and decomposed into sums of cross-correlations of weight functions via the cross-correlation, defined as

$$(f \otimes g)(\mathbf{r} = \mathbf{r}_i - \mathbf{r}_j) := \int_{\mathbb{R}} d\mathbf{r}' f(\mathbf{r}' - \mathbf{r}_i) g(\mathbf{r}' - \mathbf{r}_j) . \quad (26)$$

This can be done exactly for three-dimensional systems. However, two-dimensional systems require an infinite number of weight functions and therefore an exact decomposition fails. The Gauss-Bonnet theorem from integral geometry is applied to perform the decomposition of the Mayer function [9]. So we obtain

$$-f(\mathbf{r}) \approx \omega_2 \otimes \omega_0 + \omega_0 \otimes \omega_2 + C_0 \omega_1 \otimes \omega_1 + C_1 \boldsymbol{\omega}_1 \otimes \boldsymbol{\omega}_1 + C_2 \hat{\boldsymbol{\omega}}_1 \otimes \hat{\boldsymbol{\omega}}_1 + \dots \quad (27)$$

with the constants  $C_0 = \frac{\pi}{2}$ ,  $C_1 = -1$ ,  $C_2 = -\frac{\pi}{4}$  and the weight functions

$$\begin{aligned} \omega_2(r) &= \Theta(R - r) \\ \omega_1(r) &= \delta(R - r) \\ \omega_0(r) &= \frac{1}{2\pi R} \delta(R - r) = \frac{1}{2\pi R} \omega_1(r) \\ \boldsymbol{\omega}_1(\mathbf{r}) &= \frac{\mathbf{r}}{r} \delta(R - r) = \frac{\mathbf{r}}{r} \omega_1(r) \\ \hat{\boldsymbol{\omega}}_1(\mathbf{r}) &= \frac{\mathbf{r}\mathbf{r}}{r^2} \delta(R - r) = \frac{\mathbf{r}\mathbf{r}}{r^2} \omega_1(r) \end{aligned} \quad (28)$$

with the Dirac delta distribution  $\delta(x)$  and the radius  $R = \sigma/2$ . In the following we will refer with the index  $\nu$  to the elements in the set

$$\{\omega_\nu(\mathbf{r}) \mid \nu = 1, 2, 3, 4, 5\} = \{\omega_2(r), \omega_1(r), \omega_0(r), \boldsymbol{\omega}_1(\mathbf{r}), \hat{\boldsymbol{\omega}}_1(\mathbf{r})\} \quad (29)$$

Hereby we do not refer to individual components of the weight functions, but to the three scalar weight functions  $\omega_2(r)$ ,  $\omega_1(r)$ ,  $\omega_0(r)$ , to the vector weight function  $\boldsymbol{\omega}_1(\mathbf{r})$  and to the matrix weight function  $\hat{\boldsymbol{\omega}}_1(\mathbf{r})$ . The convolution is defined as

$$(f * g)(\mathbf{r}) := \int_{\mathbb{R}} d\mathbf{r}' f(\mathbf{r}') g(\mathbf{r} - \mathbf{r}') \quad (30)$$

and the weighted densities  $n_\nu(\mathbf{r})$  are defined as

$$n_\nu(\mathbf{r}) = (\rho * \omega_\nu)(\mathbf{r}) . \quad (31)$$

The excess free energy density can be expressed in terms of the weighted densities  $n_\nu(\mathbf{r})$  as

$$\beta \mathcal{F}_{\text{exc,hard}}[\rho(\mathbf{r})] = \int_{\mathbb{R}^2} d\mathbf{r} \Phi(\{n_\nu\}) \quad (32)$$

with the free energy density

$$\Phi(\{n_\nu(\mathbf{r})\}) = -n_0 \ln(1 - n_2) + \frac{1}{4\pi(1 - n_2)} \left[ \tilde{C}_0 (n_1)^2 + \tilde{C}_1 \mathbf{n}_1 \cdot \mathbf{n}_1 + \tilde{C}_2 \text{Tr}(\hat{\mathbf{n}}_1^2) \right] \quad (33)$$

with  $\tilde{C}_0 = \frac{19}{12}$ ,  $\tilde{C}_1 = -\frac{5}{12}$  and  $\tilde{C}_2 = -\frac{7}{6}$ .

## 2.4 Coarse-Grained Free Energy Functional for Soft Particles

In this section we will derive a coarse-grained excess free energy functional for soft particles. For soft step potential particles with diameter  $\lambda\sigma$  and height  $h$  the isotropic pair-potential is

$$\Phi_{\text{soft}}(\mathbf{r}_i, \mathbf{r}_j) = \begin{cases} h, & \text{for } |\mathbf{r}_i - \mathbf{r}_j| \leq \lambda\sigma \\ 0, & \text{for } |\mathbf{r}_i - \mathbf{r}_j| > \lambda\sigma \end{cases} \quad (34)$$

as shown in figure 4. With  $r$  as the distance  $|\mathbf{r}_i - \mathbf{r}_j|$  between the two position vectors of disk  $i$  and disk  $j$  we rewrite the potential using the theta function as

$$\Phi_{\text{soft}}(r) = h\Theta(\lambda\sigma - r). \quad (35)$$

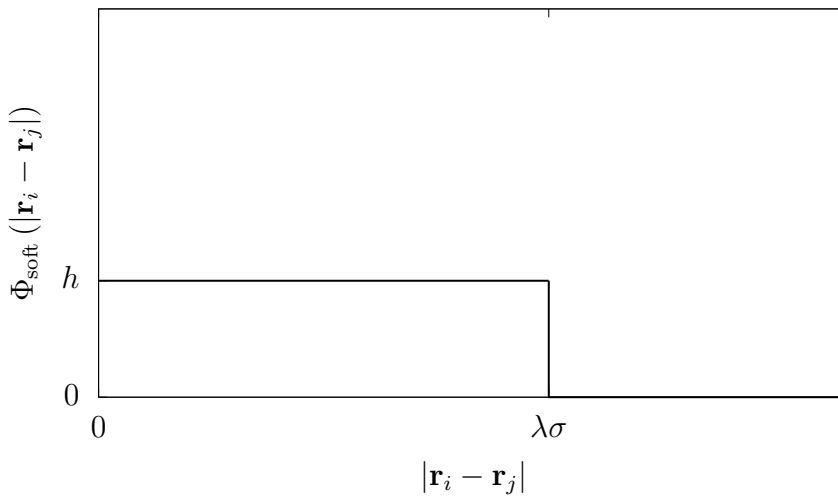


Figure 4: Potential to model the pairwise interaction between particles  $i$  and  $j$  given their positions  $\mathbf{r}_i$  and  $\mathbf{r}_j$ . This potential models particles with soft shoulders of height  $h$  and diameter  $\lambda\sigma$ . This potential is described by two independent positive real parameters  $h$  and  $\tilde{\sigma} = \lambda\sigma$  with  $\lambda > 1$ .

We start with a general effective isotropic pair-potential of the form

$$\Phi(\mathbf{r}_i, \mathbf{r}_j) = \Phi(|\mathbf{r}_i - \mathbf{r}_j|). \quad (36)$$

As introduced in section 2.1, the N-particle Hamiltonian is given by

$$H(\boldsymbol{\pi}) = T(\{\mathbf{p}_i\}) + U_{\text{int}}(\{\mathbf{r}_i\}) + U_{\text{ext}}(\{\mathbf{r}_i\}) \quad (37)$$

with the kinetic energy

$$T(\{\mathbf{p}_i\}) = \sum_{i=1}^N \frac{\mathbf{p}_i^2}{2m_i} \quad (38)$$

and the external potential energy  $U_{\text{ext}}(\{\mathbf{r}_i\}) \equiv 0$ . We will derive the mean field free energy which means that we do not consider correlation functions and multi-particle densities. Therefore the mean field approach is an approximation. The potential energy can be expressed via the grand canonical average of the microscopic one-particle density

$$\rho(\mathbf{r}) = \left\langle \sum_{i=1}^N \delta(\mathbf{r} - \mathbf{r}_i) \right\rangle \quad (39)$$

as

$$\begin{aligned} U(\{\mathbf{r}_i\}) &= \sum_{i=1}^N \sum_{j=1}^{i-1} \phi(|\mathbf{r}_i - \mathbf{r}_j|) \\ &= \frac{1}{2} \sum_{i=1}^N \sum_{j=1}^N \phi(|\mathbf{r}_i - \mathbf{r}_j|) - \frac{1}{2} \sum_{i=1}^N \phi(|\mathbf{r}_i - \mathbf{r}_i|) \\ &= \frac{1}{2} \int_{\mathbb{R}^4} d\mathbf{r} d\mathbf{r}' \rho(\mathbf{r}) \phi(|\mathbf{r} - \mathbf{r}'|) \rho(\mathbf{r}') - \frac{1}{2} N \phi(0) . \end{aligned} \quad (40)$$

Hereby we consider the self interaction of particles in the second constant term  $-\frac{1}{2}N\phi(0)$ . By rescaling the potential energy to get rid of this constant term, we obtain

$$U[\rho(\mathbf{r})] = \frac{1}{2} \int_{\mathbb{R}^4} d\mathbf{r} d\mathbf{r}' \rho(\mathbf{r}) \phi(|\mathbf{r} - \mathbf{r}'|) \rho(\mathbf{r}') . \quad (41)$$

The Helmholtz free energy is given by

$$\mathcal{F}[\rho(\mathbf{r})] = U[\rho(\mathbf{r})] - TS[\rho(\mathbf{r})] . \quad (42)$$

Since we have already considered the entropy term within the ideal gas contribution, the excess free energy functional for soft particles is

$$\mathcal{F}_{\text{exc,soft}}[\rho(\mathbf{r})] = \frac{1}{2} \int_{\mathbb{R}^4} d\mathbf{r} d\mathbf{r}' \rho(\mathbf{r}) \phi(|\mathbf{r} - \mathbf{r}'|) \rho(\mathbf{r}') . \quad (43)$$

The functional derivative of the excess soft free energy is calculated to

$$\frac{\delta \mathcal{F}_{\text{exc,soft}}[\rho(\mathbf{r})]}{\delta \rho(\mathbf{r})} = \int_{\mathbb{R}^2} d\mathbf{r}' \rho(\mathbf{r}') \phi(|\mathbf{r} - \mathbf{r}'|) = (\rho * \phi)(\mathbf{r}) , \quad (44)$$

which can be expressed as a convolution of the density field and of the potential. An alternative derivation, which is shown in [17], can be extended to more advanced approximations and leads to the same excess free energy functional for soft particles as in equation 43.

### 3 Numerical Calculations

In a nutshell, we pass the arguments in table 1 to a program, which calculates approximately the corresponding equilibrium density field  $\rho_{\text{equ}}(\mathbf{r})$  by Picard iteration. The program has been implemented in the course of this bachelor's thesis.

$\eta$	packing fraction
$\lambda$	relative diameter of soft particles
$h$	height of soft shoulders $h$
$q$	aspect ratio of the box
$N$	number of particles if there were no vacancies
$n_{\text{vac}}$	concentration of vacancies
config	initial configuration: constant, gauss or random
$N_x$	number of pixels in x-direction
$\alpha$	mixing parameter
$\Delta F$	maximal difference of free energy for break of Picard iteration

Table 1: In the first block the three physical parameters are shown. In the second block important simulation parameters and in the third block additional simulation parameters are shown.

In the following we will present the numerical procedure in detail. The numerical ideas are based on [12], [16] and [18]. For performance reasons we have chosen the programming language C++, so some references will be C++ specific. Of course, the numerical implementation could be done in any other programming language as well.

#### 3.1 Box

We start by defining a two-dimensional finite-sized rectangular box with periodic boundary conditions in both directions. This box provides the fine grid for discretising the density field  $\rho(\mathbf{r})$  to perform numerical calculations. The parameters to define the box are  $N_x$ ,  $q$ ,  $N$ ,  $n_{\text{vac}}$ ,  $\eta$ . The resolution of the box is discrete, having  $N_x$  pixels in the x-direction, each of length  $\Delta x$  and  $N_y$  pixels in the y-direction, each of length  $\Delta y$ . We decided to set  $N_x \equiv N_y$  for optimal performance of the numerical Fourier transform. The symmetry of the rectangular box with length  $L_x = N_x \Delta x$  in x-direction and length  $L_y = N_y \Delta y$  in y-direction will be defined by the length of a pixel  $\Delta x$  in x-direction and the length of a pixel  $\Delta y$  in y-direction as

$$q = \frac{L_y}{L_x} = \frac{\Delta y}{\Delta x}. \quad (45)$$

The numerical value of  $N_x$  is predefined and determined by balancing resolution and precision against computational costs. The aspect ratio  $q$  is given by the symmetry of the physical system, for instance by the unit cell of a crystal. The physical results should be independent of the chosen values for  $N_x$  as long as the resolution is sufficiently large.

For large box sizes with many particles the results should be independent of the aspect ratio of the box  $q$ . The numerical value for  $\Delta x$ , and thus also for  $\Delta y$ , will be determined in the following. Moreover we consider vacancies in our system, which are controlled by the concentration of vacancies  $\eta_{\text{vac}}$ . In two dimensions the concentration of vacancies can be relatively high compared to three dimensions. This leads to  $N(1 - n_{\text{vac}})$  particles in the box, while  $N$  is the number of particles in the box for  $\eta_{\text{vac}} = 0$ . We set the radius of the hard spheres  $R = 1$ . Therefore we have to adapt  $\Delta x$  such, that the following two equations

$$N(1 - n_{\text{vac}}) = \int_{\text{box}} d\mathbf{r} \rho(\mathbf{r}) \quad (46)$$

and

$$\eta = \frac{\pi R^2}{q(\Delta x N_x)^2} \int_{\text{box}} d\mathbf{r} \rho(\mathbf{r}) \quad (47)$$

are met. We stress that the packing fraction will be calculated with reference to the hard particles of radius  $R = 1$ . Combining these two equations we obtain the length and beam of one single pixel as

$$\begin{aligned} \Delta x &= \frac{R}{N_x} \sqrt{\frac{\pi N(1 - n_{\text{vac}})}{\eta q}} \\ \Delta y &= q\Delta x. \end{aligned} \quad (48)$$

Now all parameters for the box are available.

## 3.2 Initial Density Field

In the box we initialise the density field using the C++ vector class. There are three different groups of initial field configurations, namely constant, gauss or random. For the first one we initialise a constant density field. This procedure is preferred for the very first testing cycle. For the second one we impose a certain field configuration by setting Gaussian peaks in the box. This procedure is preferred for testing different parameters. For the third one we initialize a random field in Fourier space by setting pseudo random complex numbers up to a certain threshold wave vector. We generate the pseudo random numbers with the C++ Mersenne Twister 19937 generator. The threshold wave vector ensures smooth random fluctuations. If the wave vectors were too large, the resulting short wavelengths in real space would cause numerical problems during the minimization procedure. The third case is preferred for checking physical results, since the equilibrium density configuration should be independent of the initial field.

## 3.3 Weight Functions $\omega_\nu(\mathbf{r})$

Next, we initialize the weight functions  $\omega_\nu(\mathbf{r})$ . Since the delta distributions of infinite height and the discontinuous theta function occur in the weight functions  $\omega_\nu(\mathbf{r})$  in real

space we initialize the weight functions in Fourier space. Therefore we calculate their Fourier transform analytically via

$$\mathcal{FT}[\omega_\nu(\mathbf{r})](\mathbf{k}) = \frac{1}{2\pi} \int_{\mathbb{R}^2} \omega_\nu(\mathbf{r}) e^{-i\mathbf{k}\mathbf{r}} d\mathbf{r} \quad (49)$$

and obtain the following results

$$\begin{aligned} \mathcal{FT}[\omega_2(r)](k) &= \frac{R}{k} J_1(kR) \\ \mathcal{FT}[\omega_1(r)](k) &= RJ_0(kR) \\ \mathcal{FT}[\omega_1(r)](k) &= \frac{1}{2\pi} J_0(kR) \\ \mathcal{FT}[\omega_1(\mathbf{r})](\mathbf{k}) &= -iR \frac{\mathbf{k}}{k} J_1(kR) \\ \mathcal{FT}[\hat{\omega}_1(\mathbf{r})](\mathbf{k}) &= -R \frac{\mathbf{k}\mathbf{k}}{k^2} J_2(kR) + \frac{\hat{1}}{k} J_1(kR) \end{aligned} \quad (50)$$

with the dyadic product  $\mathbf{k}\mathbf{k}$  and the Bessel functions of first kind defined as

$$J_n(z) = \left(\frac{1}{2}z\right)^n \sum_{l=0}^{\infty} (-1)^l \frac{\left(\frac{1}{4}z^2\right)^l}{l! \Gamma(n+l+1)} \quad (51)$$

with the gamma function  $\Gamma(z) = \int_0^\infty dt e^{-t} t^{z-1}$ . For the numerical implementation of the Bessel function of first kind we use the C++ boost library. The transformation between the dimensions  $\Delta x$  and  $\Delta y$  of a pixel in real space and its dimensions  $\Delta k_x$  and  $\Delta k_y$  in Fourier space will be calculated via

$$\begin{aligned} \Delta k_x &= \frac{2\pi}{\Delta x N_x} \\ \Delta k_y &= \frac{2\pi}{\Delta y N_y}. \end{aligned} \quad (52)$$

For all numerical Fourier transformations we use a discrete Fourier transformation, provided by the C++ library FFTW3 [19]. In contrast to the continuous Fourier transform, the numerical Fourier transform is defined for a real two dimensional array  $A$  of size  $N_x \times N_y$  as

$$Y_{k,l} = \sum_{x=0}^{N_x-1} \sum_{y=0}^{N_y-1} A_{x,y} \exp\left(-2\pi i \left(\frac{xk}{N_x} + \frac{yl}{N_y}\right)\right) \quad (53)$$

with  $k \in \{0, 1, \dots, N_x - 1\}$  and  $l \in \{0, 1, \dots, N_y - 1\}$ . Therefore we have to introduce a suitable factor, here for the two dimensional case

$$\frac{2\pi}{N_x N_y \Delta x \Delta y}, \quad (54)$$

to get from the result of the continuous Fourier transform the corresponding result of the discrete Fourier transform.

### 3.4 Weight Functions $n_\nu(\mathbf{r})$

The weight functions  $n_\nu(\mathbf{r})$  are calculated via the convolution of the density field and the weights  $\omega_\nu(\mathbf{r})$ . Since a convolution becomes a multiplication in Fourier space

$$\mathcal{FT}(f * g) = \mathcal{FT}(f) \mathcal{FT}(g) , \quad (55)$$

it is faster to perform convolutions via a numerical Fourier transform in Fourier space. Therefore we will multiply the numerical Fourier transform of the density field with the analytical Fourier transform of the weight functions. In a further step, we will calculate the inverse Fourier transform of the latter result

$$n_\nu(\mathbf{r}) = \mathcal{FT}^{-1}\left(\mathcal{FT}[\rho(\mathbf{r})](\mathbf{k}) \mathcal{FT}[\omega_\nu(\mathbf{r})](\mathbf{k})\right) . \quad (56)$$

### 3.5 Weight Functions $T_\nu(\mathbf{r})$

We calculate the weight functions  $T_\nu(\mathbf{r})$  via

$$T_\nu = \frac{\delta\Phi}{\delta n_\nu(\mathbf{r})} \quad (57)$$

with the free energy density

$$\Phi(\{n_\nu(\mathbf{r})\}) = -n_0 \ln(1 - n_2) + \frac{1}{4\pi(1 - n_2)} \left[ \tilde{C}_0 (n_1)^2 + \tilde{C}_1 \mathbf{n}_1 \cdot \mathbf{n}_1 + \tilde{C}_2 \text{Tr}(\hat{\mathbf{n}}_1^2) \right] \quad (58)$$

with  $\tilde{C}_0 = \frac{19}{12}$ ,  $\tilde{C}_1 = -\frac{5}{12}$  and  $\tilde{C}_2 = -\frac{7}{6}$ . Thereby we obtain the following results

$$\begin{aligned} T_2(\mathbf{r}) &= \frac{n_0}{1 - n_2} + \frac{1}{4\pi(1 - n_2)^2} \left( \frac{19}{12} (n_1)^2 - \frac{5}{12} \mathbf{n}_1 \cdot \mathbf{n}_1 - \frac{7}{6} \text{Tr}(\hat{\mathbf{n}}_1^2) \right) \\ T_1(\mathbf{r}) &= \frac{19}{24\pi(1 - n_2)} n_1 \\ T_0(\mathbf{r}) &= -\ln(1 - n_2) \\ \mathbf{T}_1(\mathbf{r}) &= -\frac{5}{24\pi(1 - n_2)} \mathbf{n}_1 \\ \left(\hat{\mathbf{T}}_1(\mathbf{r})\right)_{xx} &= -\frac{7}{12\pi(1 - n_2)} (\hat{\mathbf{n}}_1)_{xx} \\ \left(\hat{\mathbf{T}}_1(\mathbf{r})\right)_{xy} &= -\frac{7}{6\pi(1 - n_2)} (\hat{\mathbf{n}}_1)_{xy} \\ \left(\hat{\mathbf{T}}_1(\mathbf{r})\right)_{yy} &= -\frac{7}{12\pi(1 - n_2)} (\hat{\mathbf{n}}_1)_{yy} , \end{aligned} \quad (59)$$

in which we insert the the weight functions  $n_\nu(\mathbf{r})$ .

### 3.6 Functional Derivative of Excess Free Energy for Hard Particles

The functional derivative of the excess free energy functional can be expressed through a convolution, which simplifies the calculation to

$$\begin{aligned}
\frac{\delta (\beta \mathcal{F}_{\text{exc,hard}} [\rho (\mathbf{r})])}{\delta \rho (\mathbf{r})} &= \int_{\mathbb{R}^2} d\mathbf{r}' \frac{\delta \Phi}{\delta \rho (\mathbf{r})} \\
&= \sum_{\nu} \int_{\mathbb{R}^2} d\mathbf{r}' \frac{\delta \Phi}{\delta n_{\nu} (\mathbf{r}')} \frac{\delta n_{\nu} (\mathbf{r}')}{\delta \rho (\mathbf{r})} \\
&= \sum_{\nu} \int_{\mathbb{R}^2} d\mathbf{r}' T_{\nu} (\mathbf{r}) \omega_{\nu} (\mathbf{r}' - \mathbf{r}) \\
&= \sum_{\nu} \int_{\mathbb{R}^2} d\mathbf{r}' T_{\nu} (\mathbf{r}) \xi_{\nu} \omega_{\nu} (\mathbf{r} - \mathbf{r}') \\
&= \sum_{\nu} \xi_{\nu} (T_{\nu} * \omega_{\nu}) (\mathbf{r}) ,
\end{aligned} \tag{60}$$

whereby  $\xi_{\nu}$  equals 1 for symmetric and  $-1$  for antisymmetric weight functions  $\omega_{\nu} (\mathbf{r})$ . In our case the vector weight function  $\omega_1 (\mathbf{r})$  is the only antisymmetric weight function. Finally, we will calculate the functional derivative of the excess free energy for hard particles via a sum of convolutions in Fourier space

$$\frac{\delta (\beta \mathcal{F}_{\text{exc,hard}} [\rho (\mathbf{r})])}{\delta \rho (\mathbf{r})} = \sum_{\nu} \xi_{\nu} \mathcal{F}\mathcal{T}^{-1} \left( \mathcal{F}\mathcal{T} [T_{\nu} (\mathbf{r})] (\mathbf{k}) \mathcal{F}\mathcal{T} [\omega_{\nu} (\mathbf{r})] (\mathbf{k}) \right) . \tag{61}$$

### 3.7 Functional Derivative of Excess Free Energy for Soft Particles

In order to calculate numerically the functional derivative of the excess free energy for soft square particles with a step potential via mean field theory, we need the two parameters  $\lambda$  and  $h$ . The functional derivative of the excess soft free energy is

$$\frac{\delta (\beta \mathcal{F}_{\text{exc,soft}} [\rho (\mathbf{r})])}{\delta \rho (\mathbf{r})} = \beta \int_{\mathbb{R}^2} d\mathbf{r}' \rho (\mathbf{r}') \phi (|\mathbf{r} - \mathbf{r}'|) = \beta (\rho * \phi) (\mathbf{r}) \tag{62}$$

where  $r$  denotes the distance  $|\mathbf{r}_i - \mathbf{r}_j|$  between the two position vectors of disk  $i$  and disk  $j$  and  $\sigma = 2$  the diameter of hard particles the potential is given as

$$\phi (|\mathbf{r} - \mathbf{r}'|) = \phi (r) = h \Theta (\lambda \sigma - r) . \tag{63}$$

Since the potential function contains the unsteady theta function we will initialize the potential in Fourier space. Its analytical Fourier transform is given as

$$\mathcal{F}\mathcal{T} [\Phi (r)] (k) = \frac{h \lambda \sigma}{k} J_1 (k \lambda \sigma) \tag{64}$$

with  $J_n(z)$  the Bessel functions of first kind defined in equation 51. Finally we will calculate the functional derivative of the excess free energy for soft particles via a convolution in Fourier space

$$\frac{\delta(\beta\mathcal{F}_{\text{exc,soft}}[\rho(\mathbf{r})])}{\delta\rho(\mathbf{r})} = \beta\mathcal{FT}^{-1}\left(\mathcal{FT}[\rho(\mathbf{r})](\mathbf{k}) \mathcal{FT}[\Phi(r)](\mathbf{k})\right). \quad (65)$$

### 3.8 Picard Iteration

In the following we will describe how to minimize  $\Omega[\rho(\mathbf{r})]$  through Picard iteration, which is a fixed-point iteration for ordinary differential equations. The parameters for Picard iteration are  $\alpha$  and  $\Delta F$ . The minimization of  $\Omega[\rho(\mathbf{r})]$  leads to the following equation

$$\rho(\mathbf{r}) = \frac{1}{\Lambda^2} \exp\left(-\frac{\delta(\beta\mathcal{F}_{\text{exc,hard}}[\rho(\mathbf{r})])}{\delta\rho(\mathbf{r})} - \frac{\delta(\beta\mathcal{F}_{\text{exc,soft}}[\rho(\mathbf{r})])}{\delta\rho(\mathbf{r})} - \beta V(\mathbf{r}) + \beta\mu\right). \quad (66)$$

So far we have already shown how to calculate the functional derivatives of the excess free energy functional for hard and soft particles. We set  $\Lambda \equiv 1$  and  $V(\mathbf{r}) \equiv 0$  since we do not consider any external potential. Therefore the equation for  $\rho(\mathbf{r})$  simplifies to

$$\begin{aligned} \rho(\mathbf{r}) &= \exp\left(-\frac{\delta(\beta\mathcal{F}_{\text{exc,hard}}[\rho(\mathbf{r})])}{\delta\rho(\mathbf{r})} - \frac{\delta(\beta\mathcal{F}_{\text{exc,soft}}[\rho(\mathbf{r})])}{\delta\rho(\mathbf{r})} + \beta\mu\right) \\ &= \exp(c^{(1)}(\mathbf{r}) + \beta\mu), \end{aligned} \quad (67)$$

whereby we have rewritten the functional derivative of the excess free energy functional a direct correlation function in the last step. As an initial step, we once initialize the box and the initial density field  $\rho_0(\mathbf{r})$  as described in sections 3.1 and 3.2.

The Picard iteration consists of four steps which are applied repeatedly. As step number one we calculate

$$\rho_{i+1}(\mathbf{r}) \exp(-\beta\mu'_{i+1}) = \exp(c^{(1)}(\mathbf{r})) \quad (68)$$

as described in sections 3.3 to 3.7. As step number two we multiply the result with  $\exp(\beta\mu'_{i+1})$  such that

$$\int_{\text{box}} d\mathbf{r} \rho'_{i+1}(\mathbf{r}) = \int_{\text{box}} d\mathbf{r} \exp(c^{(1)}(\mathbf{r}) + \beta\mu'_{i+1}) = N(1 - n_{\text{vac}}) \quad (69)$$

is satisfied. This ensures the conservation of the number of particles in our box. As step number three we mix the new density field with the old density field with the mixing parameter  $\alpha \in [0, 1]$  as

$$\rho_{i+1}(\mathbf{r}) = \alpha\rho'_{i+1}(\mathbf{r}) + (1 - \alpha)\rho_i(\mathbf{r}) \quad (70)$$

in order to avoid rapid changes which might lead to numerical problems and unphysical results. As step number four we continue calculating the density field for the next iteration. The process is repeated until the result converges. We stop the Picard iteration if the difference between the free energy of iteration step  $i$  and  $i + 1$  is smaller than  $\Delta F$ . We denote the final step  $j$ . As a final result we obtain the density field  $\rho_j(\mathbf{r})$  as an approximation of the equilibrium density field for the given physical parameters  $\eta$ ,  $\lambda$  and  $h$ .

## 4 Results

In this section we will present our results as we advance from numerical test cases for density functional theory to physical test cases for hard particles and soft particles. As a final step we consider particles with hard cores and soft shoulders. This procedure ensures step-by-step testing while developing the program.

### 4.1 Test Case: Weight Functions $\omega_\nu(\mathbf{r})$

As a first test case we check the initialisation of the weight functions  $\omega_\nu(\mathbf{r})$  and the calculations involving the analytical and numerical Fourier transform. Therefore we perform the inverse discrete Fourier transform of the analytically obtained weight functions in Fourier space, shown in equation 50, and plot the results in real space as shown in figure 5. Due to the finite number of wave vectors in the discrete Fourier transform, Fourier ripples are visible.

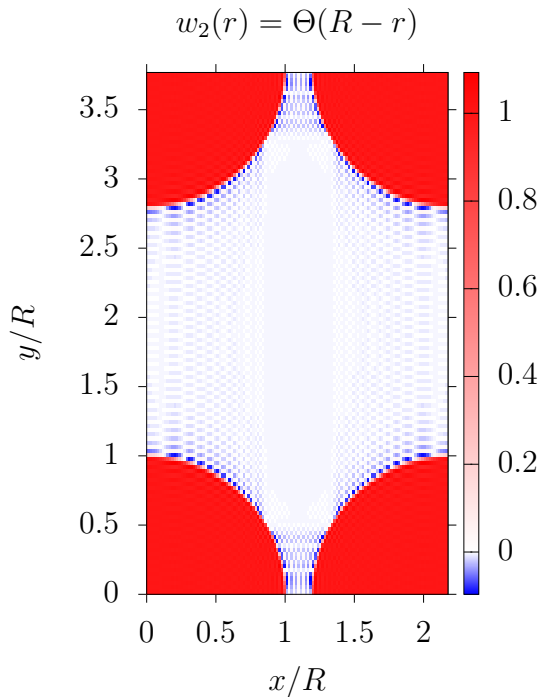


Figure 5: Weight function  $\omega_2(r) = \Theta(R - r)$  with  $r = \sqrt{x^2 + y^2}$  under periodic boundary conditions.

We calculate the integral of them in the unit cell analytically

$$\int_{\text{box}} d\mathbf{r} \omega_\nu(\mathbf{r}) \quad (71)$$

and compare the results against the numerical results

$$\Delta x \Delta y \sum_{i=0}^{N_x-1} \sum_{j=0}^{N_y-1} \omega_{\nu,i,j}. \quad (72)$$

For the weight function  $\omega_2(\mathbf{r})$  we obtain

$$\int_{\text{box}} d\mathbf{r} \omega_2(\mathbf{r}) = \int_{\text{box}} d\mathbf{r} \Theta(R-r) = \pi R^2 = \pi. \quad (73)$$

The results are shown in table 2. Within the numerical precision the numerical and analytical results agree. The values differ in the fifteenth significant digit. We obtained analog results for all other weight functions. In the appendix the components of the remaining weight functions  $\omega_{\nu}(\mathbf{r})$  are shown in figures 14 and 15.

analytically	3.141592653589793116
numerically	3.141592653589787787

Table 2: Analytical and numerical calculation of the integral over the box of  $\omega_2(\mathbf{r}) = \Theta(R-r)$  using equations 71 and 72.

## 4.2 Test Case: Constant Density Field

For a homogenous density field  $\rho(\mathbf{r}) \equiv \rho_{\text{bulk}}$ , the entire Picard iteration can be calculated analytically. So we obtain for the weight functions  $n_{\nu}(\mathbf{r})$  the following results

$$\begin{aligned} n_{2,\text{bulk}} &= \pi R^2 \rho_{\text{bulk}} \\ n_{1,\text{bulk}} &= 2\pi R \rho_{\text{bulk}} \\ n_{0,\text{bulk}} &= \rho_{\text{bulk}} \\ (\mathbf{n}_{1,\text{bulk}})_x &= (\mathbf{n}_{1,\text{bulk}})_y = 0 \\ (\hat{\mathbf{n}}_{1,\text{bulk}})_{xx} &= (\hat{\mathbf{n}}_{1,\text{bulk}})_{yy} = \pi R \rho_{\text{bulk}} \\ (\hat{\mathbf{n}}_{1,\text{bulk}})_{xy} &= (\hat{\mathbf{n}}_{1,\text{bulk}})_{yx} = 0, \end{aligned} \quad (74)$$

which we check against the numerical results for the first iteration step. Those results can be put into equation 59 to obtain the weighted function  $T_{\nu}(\mathbf{r})$ . Within the numerical precision we obtained for the numerical and analytical calculations of  $n_{\nu}(\mathbf{r})$  and  $T_{\nu}(\mathbf{r})$  the same results.

Minimizing a constant density field results always in the same constant density field, even if the packing fraction is above the freezing transition. This is not the correct physical behaviour, for which one expects a solid equilibrium density field. One obtains this unphysical result, since Picard iterations of fundamental measure theory do not change a constant field at all.

### 4.3 Test Case: Freezing Transition of Hard Disks in Two Dimensions

In the first physically relevant testcase we reproduce the freezing transition of hard disks in two dimensions via density functional theory as researched in [9]. In two dimensions hard disks freeze into a triangular phase. In figure 6 the unit cell of this triangular phase for close-packed disks with diameter  $\sigma$  is shown.

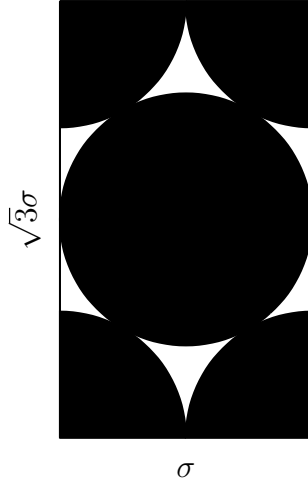


Figure 6: Unit cell of size  $\sigma$  times  $\sqrt{3}\sigma$  for close-packed disks with diameter  $\sigma$  in the triangular phase.

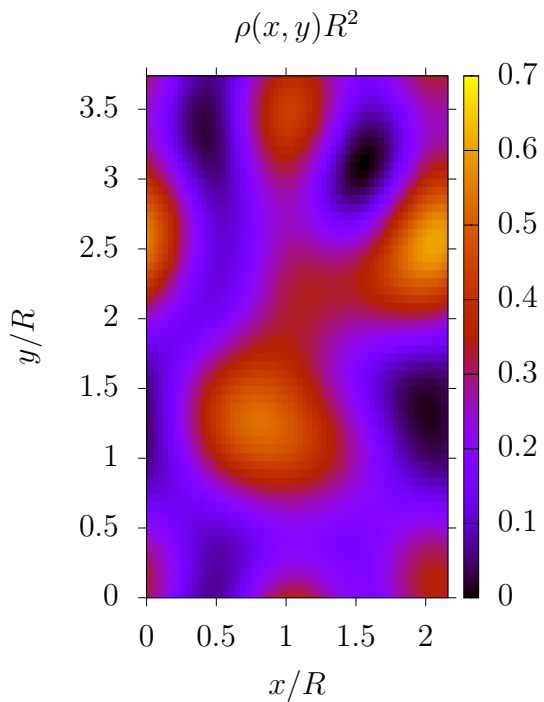
The packing fraction of close-packed disks in two dimensions is

$$\eta = \frac{\pi}{2\sqrt{3}} \approx 0.907. \quad (75)$$

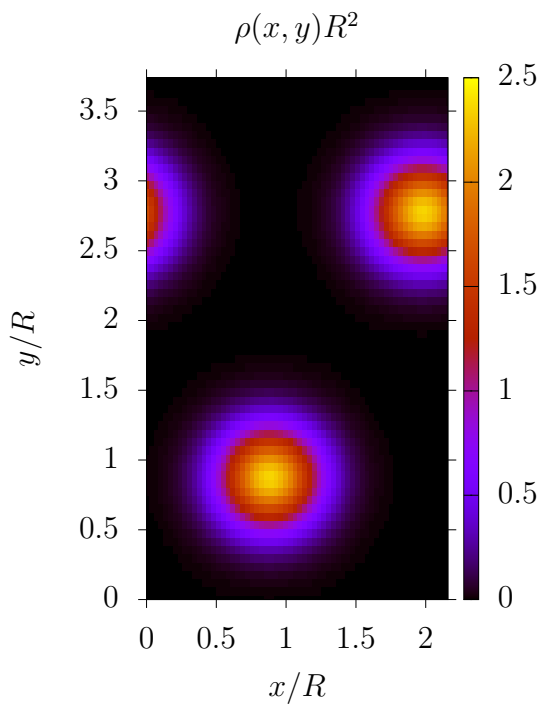
For the phase transition calculations we have chosen  $N = 2$ ,  $n_{\text{vac}} = 0.00558$ , and  $q = \sqrt{3}$ . In order to test the entropically driven fluid-solid phase transition, we analyse the equilibrium phase in dependency of the packing fraction  $\eta$ . Up to a packing fraction of  $\eta \leq 0.73$  the equilibrium density profile is liquid. For a packing fraction  $0.74 \leq \eta \leq 0.88$  the equilibrium density profile is a solid triangular phase as shown for  $\eta = 0.75$  in figure 7. For a packing fraction  $0.89 \leq \eta \leq 0.91$  the calculations suffer numerical problems. Those problems are caused by the term  $T_0(\mathbf{r}) = -\ln(1 - n_2)$  which becomes undefined for  $n_2 \geq 1$ . One possible solution is to cut-off  $n_2$  if  $n_2 \geq 1$ .

We determine the liquid-solid phase transition at  $\eta = 0.74$  which is in the same region as the result  $\eta = 0.72$  obtained in [9].

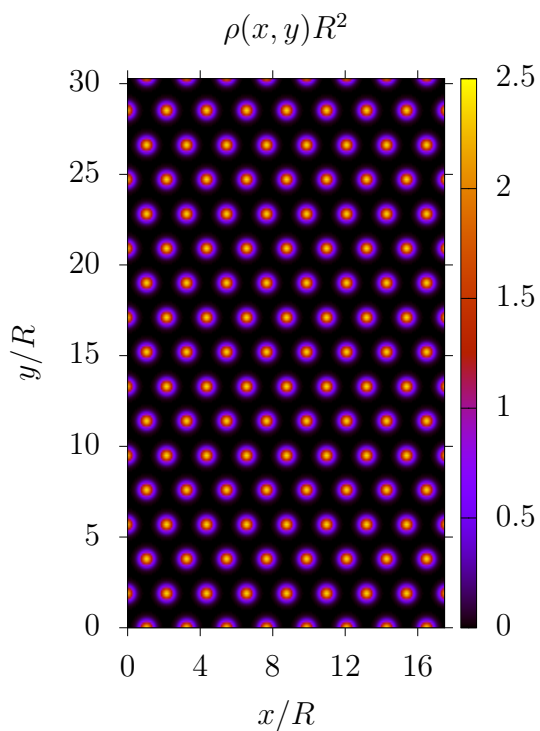
In order to test the stability of the numerical calculations we increase the size of the system to  $8 \times 8$  unit cells with a total of about 128 particles. While for particle simulation 128 particles are a small system, for density functional theory this system is quite large. As shown in figure 7c, we obtain the triangular phase as expected.



(a) Initial random density field for  $N = 2$



(b) Equilibrium density field for  $N = 2$



(c) Equilibrium density field for  $N = 128$

Figure 7: Hard disks in two dimensions. The physical parameter for all three plots is  $\eta = 0.75$  and the simulation parameters are  $n_{\text{vac}} = 0.00558$ ,  $q = \sqrt{3}$  and a random initial configuration.

## 4.4 Test Case: Freezing Transition of Soft Disks in Two Dimensions

As done before for hard particles, we will test the soft particles individually. A suitable test case is the fluid-solid phase transition.

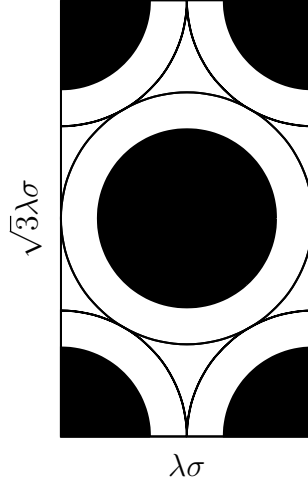


Figure 8: Unit cell of size  $\lambda\sigma$  times  $\sqrt{3}\lambda\sigma$  for close-packed disks with diameter  $\lambda\sigma$  in the triangular phase.

The packing fraction of closed packed disks interacting via a diameter  $\lambda\sigma$  with respect to a packing fraction given by the hard disk diameter  $\sigma$  is

$$\eta = \frac{\pi}{4\sqrt{3}} \approx 0.453. \quad (76)$$

For the phase transition calculations we have chosen  $N = 2$ ,  $n_{\text{vac}} = 0.00558$ , and  $q = \sqrt{3}$ . Now, in contrast to hard particles, we have two physical parameters  $h$  and  $\eta$ .

First, we analyse the equilibrium phase in dependency of the packing fraction  $\eta$  for a fixed height  $h = 6$ . The height of the soft shoulders defines the temperature  $T$  in our system as  $T \propto h^{-1}$ . For  $\eta \leq 0.18$  we obtain the fluid phase and for  $0.19 \leq \eta \leq 0.30$  the solid triangular phase as shown in figure 9. For  $0.31 \leq \eta \leq 0.45$  we obtain a solid stripe phase.

Second, we analyse the equilibrium phase in dependency of the soft shoulder height  $h$  for a fixed packing fraction  $\eta = 0.26$ . For  $h \leq 3$  we obtain the fluid phase and for  $h \geq 4$  the solid triangular phase.

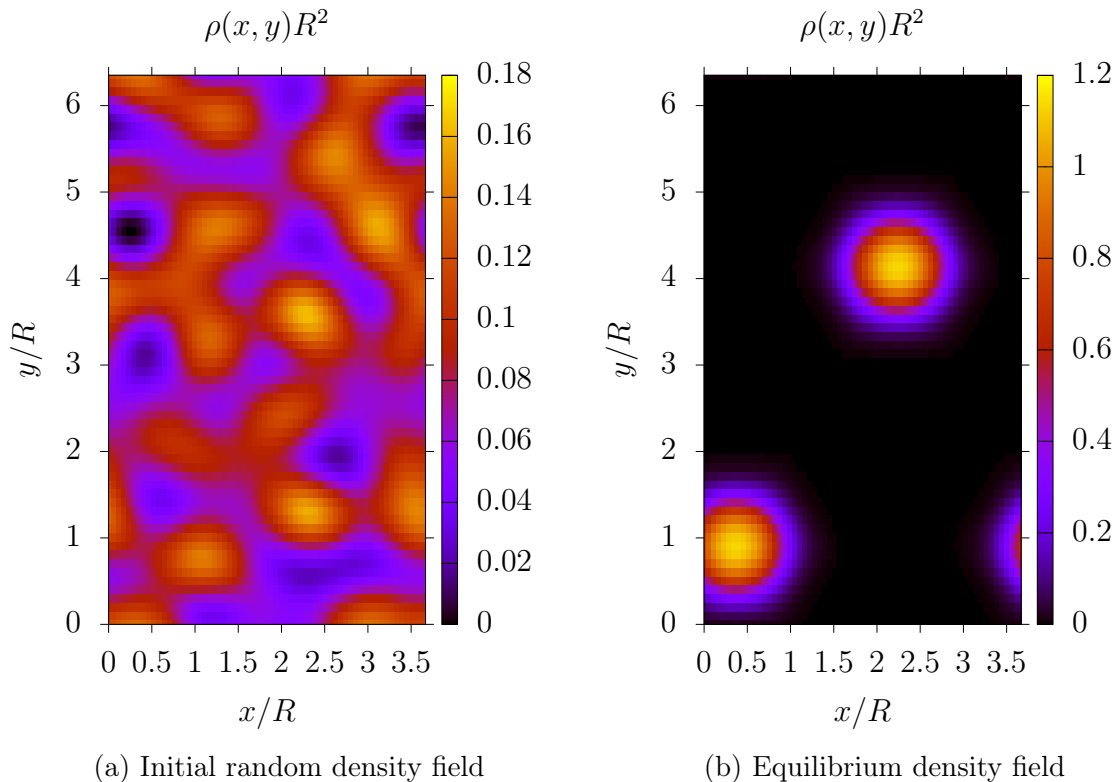


Figure 9: Unit cell of initial density field set with random initial configurations. The physical parameters are  $\eta = 0.26$ ,  $h = 6$ ,  $\lambda = \sqrt{2}$  and the simulation parameters are  $N = 2$ ,  $n_{\text{vac}} = 0.00558$   $q = \sqrt{3}$ .

## 4.5 Hard Core and Soft Shoulders

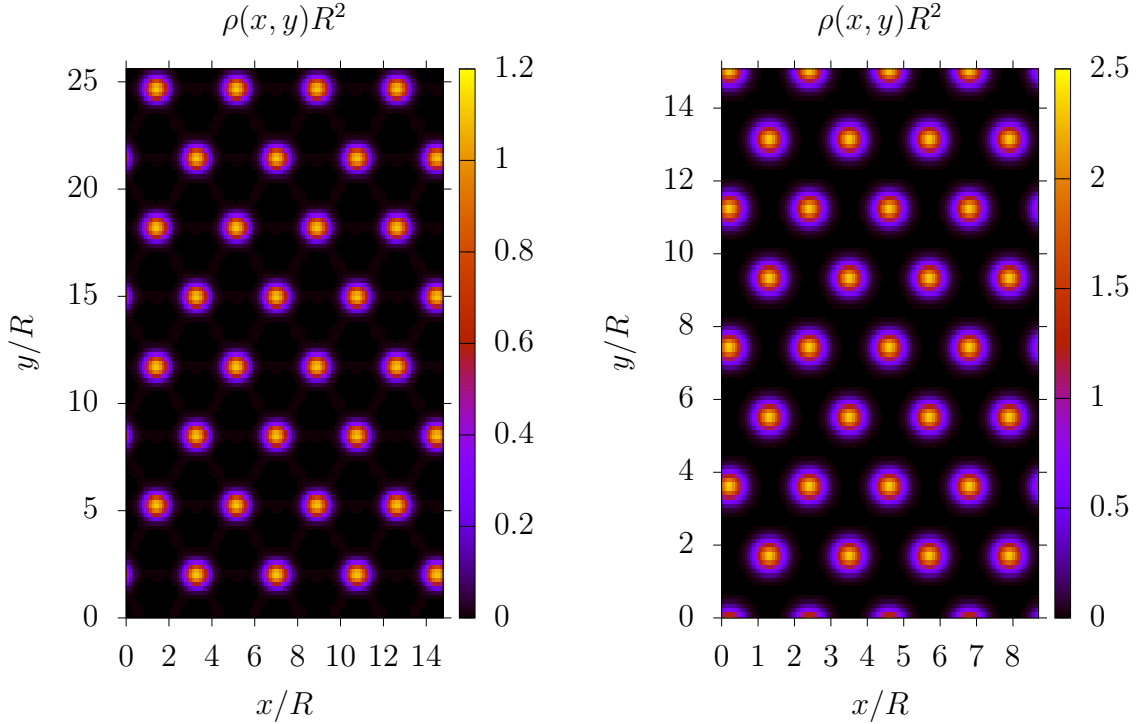
For particles with hard cores and soft square shoulders we recover the results as above. Soft shoulders with a large height  $h$  act as effectively hard particles of diameter  $\lambda\sigma$ , which leads to a triangular solid phase as shown in figure 10a. In contrast, soft shoulders with a small height are negligible and act as effectively hard particles of diameter  $\sigma$  as shown in figure 10b. Both extreme cases were found. Moreover they are stable for larger systems as shown in figure 10. This shows that the implemented program for particles with hard cores and soft shoulders works correctly.

Since we have two length scales, the formation of quasiperiodic crystals might be possible. Another non-triangular phase is the quadratic phase, stabilised by two length scales as shown in figure 11. The packing fraction of this configuration is

$$\eta = \frac{\pi}{4} \approx 0.785. \quad (77)$$

The second length scale is chosen  $\lambda = \sqrt{2}$ , such that the hard cores touch each other at the sides and the soft cores touch each other at the diagonal. The idea to determine the

parameters for a quadratic phase is to start in the triangular phase with soft particles acting as effectively hard particles and to increase the packing fraction until the soft shoulders overlap on the sides and touch on the diagonal. Due to limited time we were not able to find appropriate parameters.



(a) Equilibrium density field with physical parameters  $\eta = 0.26$ ,  $h = 6$ ,  $\lambda = \sqrt{2}$ .

(b) Equilibrium density field with physical parameters  $\eta = 0.75$ ,  $h = 10^{-8}$ ,  $\lambda = \sqrt{2}$ .

Figure 10: Equilibrium density field for hard disks with soft step shoulders. The simulation parameters are  $N = 32$ ,  $n_{\text{vac}} = 0.00558$   $q = \sqrt{3}$  and a random initial configuration.

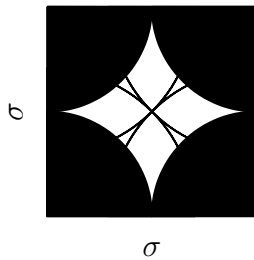


Figure 11: Unit cell of size  $\sigma$  times  $\sigma$  for disks with diameter  $\sigma$  in the quadratic phase.

## 4.6 Interesting Patterns

In this section we will present some interesting patterns obtained by our model system. However, these patterns require further analysis in order to draw physical conclusions. The Picard iteration for the parameters of the density field shown in figure 12 broke due to numerical reasons, probably caused by the weight function  $n_2$  as explained above in section 4.3.

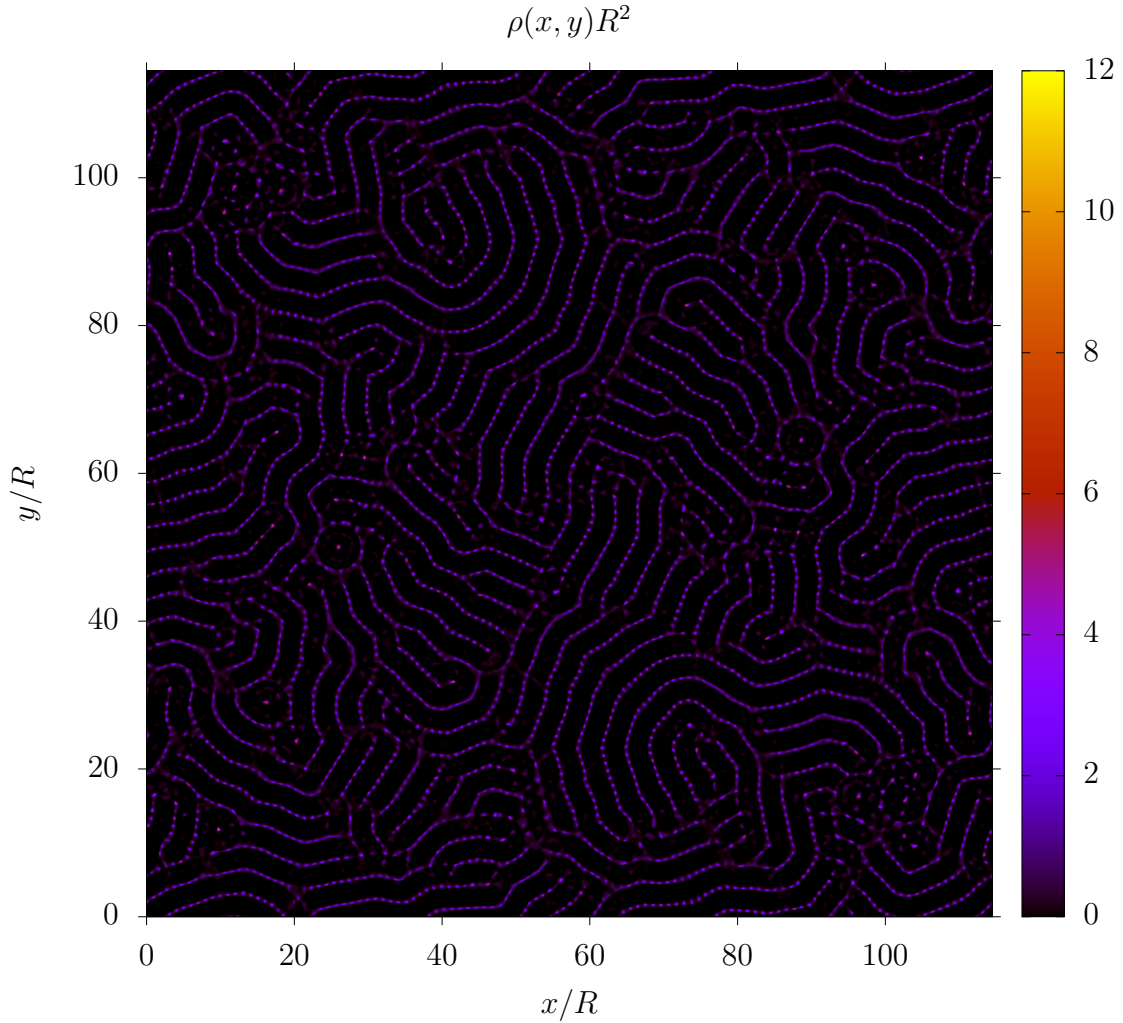


Figure 12: Density field with physical parameters  $\eta = 0.49$ ,  $h = 11.3$ ,  $\lambda = 2.86$  and simulation parameters  $N = 2048$ ,  $\eta_{\text{vac}} = 0$ ,  $q = 1$  and a random initial configuration.

The density field as shown in figure 13 shows particle positions which are closer than  $\sigma = 2$ , which is impossible for impenetrable particles. Therefore we assume that we see a superposition of different configurations in different unit cells.

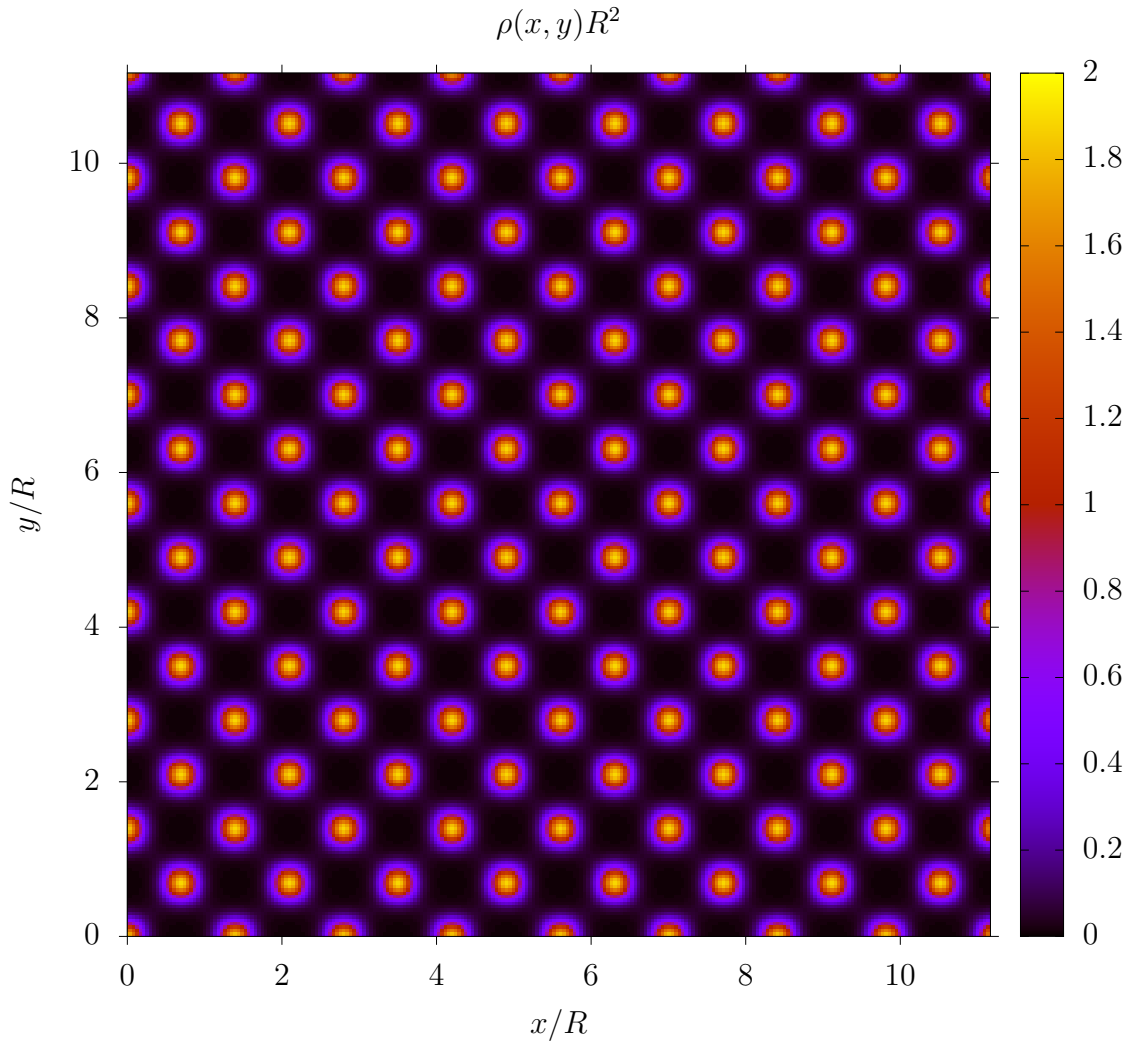


Figure 13: Equilibrium density field with physical parameters  $\eta = 0.80$ ,  $h = 4$ ,  $\lambda = \sqrt{2}$  and simulation parameters  $N = 32$ ,  $\eta_{\text{vac}} = 0$ ,  $q = 1$  and a random initial configuration.

## 5 Resume and Outlook

In this bachelor's thesis we have provided an introductory summary of density functional theory and fundamental measure theory. Moreover we have implemented density functional theory for hard disks with soft square shoulders in two dimensions. This system is described by the three physical parameters packing fraction, relative diameter of soft particles with respect to hard particles and height of soft shoulders. As the main results we have recovered the liquid-solid phase transition for hard particles and for soft particles.

With this apparatus one will be able to study the parameter space in detail and a variety of further effects by including external potentials. The next step for future work is to look for the quadratic phase and quasiperiodic crystals. This would be the first time to observe quasicrystals with hard-core particles using density functional theory.

## 6 References

- [1] P.-G. de Gennes. Nobel lecture: Soft matter. *World Scientific Publishing Co., Singapore, 1997*.
- [2] Masao Doi. *Soft Matter Physics*. Oxford University Press, August 2013.
- [3] P. Hohenberg and W. Kohn. Inhomogeneous electron gas. *Phys. Rev.*, 136:B864–B871, Nov 1964.
- [4] W. Kohn. Nobel lecture: Electronic structure of matter – wave functions and density functionals. *World Scientific Publishing Co., Singapore, 2003*.
- [5] N. David Mermin. Thermal properties of the inhomogeneous electron gas. *Phys. Rev.*, 137:A1441–A1443, Mar 1965.
- [6] Yaakov Rosenfeld. Free-energy model for the inhomogeneous hard-sphere fluid mixture and density-functional theory of freezing. *Phys. Rev. Lett.*, 63:980–983, Aug 1989.
- [7] A. J. Archer. Density functional theory for the freezing of soft-core fluids. *Phys. Rev. E*, 72:051501, Nov 2005.
- [8] E. Kierlik and M. L. Rosinberg. Density-functional theory for inhomogeneous fluids: Adsorption of binary mixtures. *Phys. Rev. A*, 44:5025–5037, Oct 1991.
- [9] Roland Roth, Klaus Mecke, and Martin Oettel. Communication: Fundamental measure theory for hard disks: Fluid and solid. *The Journal of Chemical Physics*, 136(8):081101, 2012.
- [10] P. Tarazona and Y. Rosenfeld. From zero-dimension cavities to free-energy functionals for hard disks and hard spheres. *Phys. Rev. E*, 55:R4873–R4876, May 1997.
- [11] P. Tarazona and Y. Rosenfeld. *Free Energy Density Functional from 0D Cavities*, pages 293–302. Springer Netherlands, Dordrecht, 1999.
- [12] Tim Neuhaus. *Density Functional Theory for colloidal spheres in various external potentials*. PhD thesis, 2013.
- [13] Tim Neuhaus, Andreas Härtel, M Marechal, Michael Schmiedeberg, and Hartmut Löwen. Density functional theory of heterogeneous crystallization. *The European Physical Journal Special Topics*, 223, 08 2014.
- [14] R. Roth. Fundamental measure theory of hard-sphere mixtures: a review. *J. Phys.: Condens. Matter*, 22:063102–1–18, 2010.
- [15] M. Schmiedeberg. Vorlesungsnotizen tp4: Statistische physik und thermodynamik, 2019.

- [16] R. Roth. Introduction to density functional theory of classical systems: Theory and applications, November 2006.
- [17] Samuel Savitz, Mehrtash Babadi, and Ron Lifshitz. Multiple-scale structures: from faraday waves to soft-matter quasicrystals. *IUCrJ*, 5(3):247–268, Mar 2018.
- [18] M. Oettel, S. Görig, A. Härtel, H. Löwen, M. Radu, and T. Schilling. Free energies, vacancy concentrations, and density distribution anisotropies in hard-sphere crystals: A combined density functional and simulation study. *Phys. Rev. E*, 82:051404, Nov 2010.
- [19] Matteo Frigo and Steven G. Johnson. The design and implementation of FFTW3. *Proceedings of the IEEE*, 93(2):216–231, 2005. Special issue on “Program Generation, Optimization, and Platform Adaptation”.

## 7 Appendix

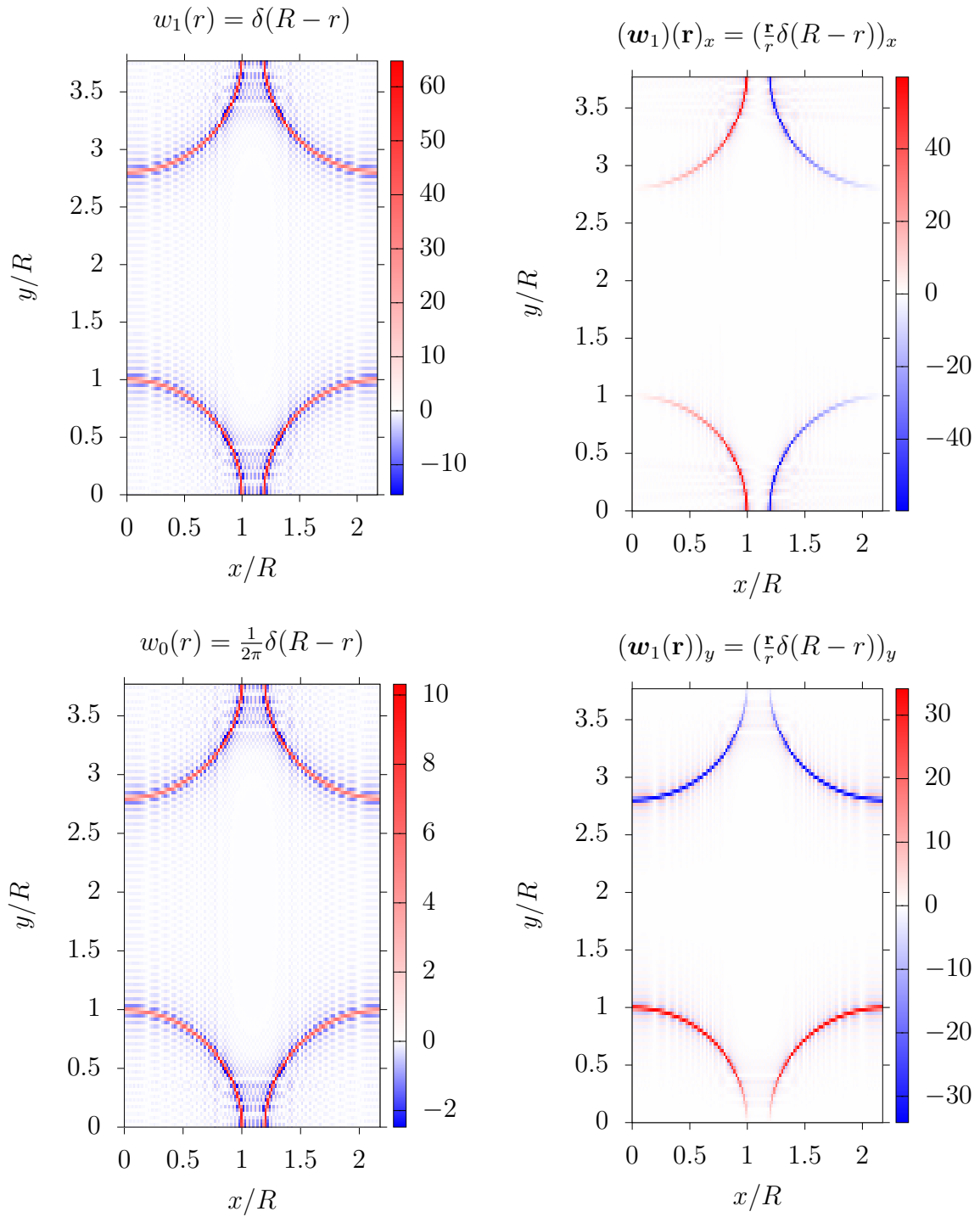


Figure 14: Weight functions  $\omega_\nu(\mathbf{r})$  - figure 1 of 2.

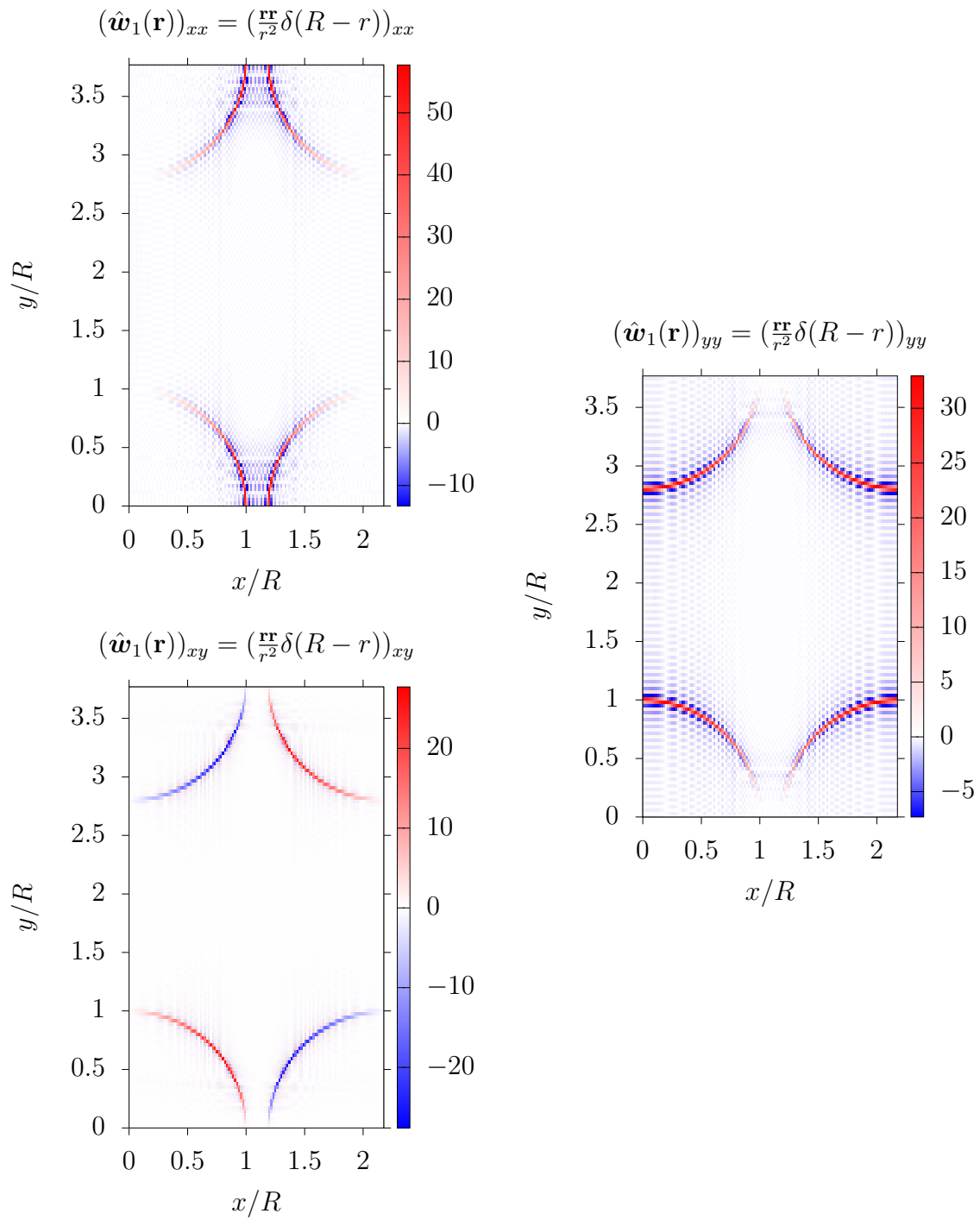


Figure 15: Weight functions  $\omega_\nu(\mathbf{r})$  - figure 2 of 2.

## Erklärung

Hiermit versichere ich, dass ich die vorliegende Arbeit selbstständig verfasst und keine anderen als die angegebenen Quellen und Hilfsmittel benutzt habe, dass alle Stellen der Arbeit, die wörtlich oder sinngemäß aus anderen Quellen übernommen wurden, als solche kenntlich gemacht sind und dass die Arbeit in gleicher oder ähnlicher Form noch keiner Prüfungsbehörde vorgelegt wurde.

Erlangen, den 22.10.2019

---